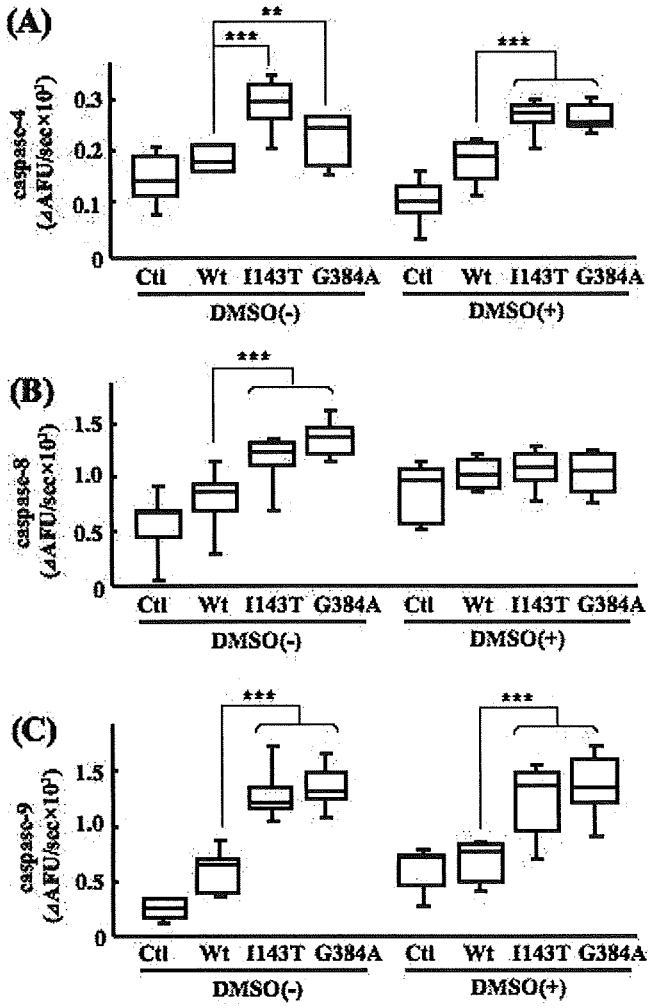

Fig. 2. Baseline activities of caspase-4, -8 and -9 in control (Ctl), wild-type PS1-transfected (Wt) and mutant PS1-transfected (I143T or G384A) cells. (A) Caspase-4 activity. (B) Caspase-8 activity. (C) Caspase-9 activity. The left panels show the activities without DMSO, while the right panels show the levels in the presence of 0.1% DMSO. Note that DMSO lowers caspase-8 activity. $^{**}p < 0.001$; $^{***}p < 0.0001$.

hibitor [28]. The BACE inhibitor (0, 2.5, and 5 μM) or γ-secretase inhibitor (0, 5, and 10 μM) was added at the same time as treatment with the apoptosis-inducing agents at each appropriate concentration. Relative cell viabilities were expressed according to the corresponding viability of each cell type without secretase inhibitor treatment. Relative caspase-3/7 activities were expressed according to the corresponding activities in control cells without secretase inhibitors.

Statistical analysis

All data obtained from six independent experiments ($n = 6$) were expressed as the mean ± SD. Differences between two groups were analyzed statistically by an unpaired two-tailed Student's t-test. For multiple comparisons, two-factor ANOVA followed by Bonferroni post-hoc analysis was performed using the StatView software. Each significance was expressed as $^{*}p < 0.01$, $^{**}p < 0.001$ or $^{***}p < 0.0001$.

RESULTS

Mutant PS1 promotes apoptosis and enhances caspase-3/7 activation

Successful transfection was confirmed by western blot in our other report [26]. Baseline cell viability and caspase-3/7 activity were not different among the

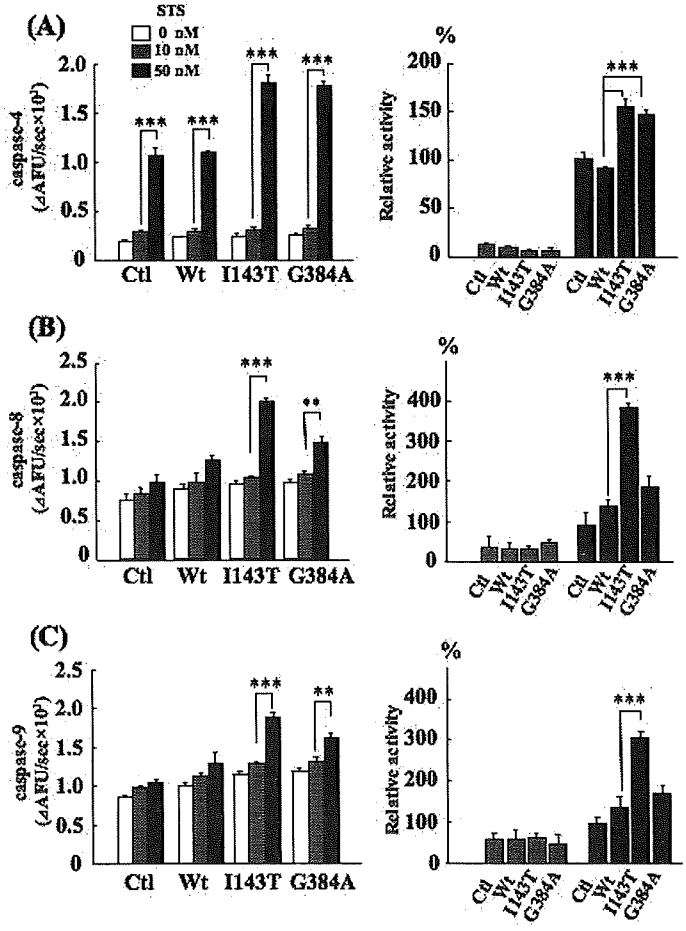

Fig. 3. Activities of caspase-4, -8 and -9 in control (Ctl), wild-type PS1-transfected (Wt), and mutant PS1-transfected (I143T or G384A) cells after treatment with STS for 6 h. (A) Caspase-4 activity. (B) Caspase-8 activity. (C) Caspase-9 activity. The left panels show the individual activities, while the right panels show the relative activities to the activities in control cells treated with 50 nM STS.** $p < 0.001$; *** $p < 0.0001$.

cell types (data not shown). At the late stage of apoptosis, cell viability was markedly decreased and did not differ among the cell types. Thus, after treatment with apoptosis-inducing agents at appropriate concentrations, we checked the cell viabilities and caspase-3/7 activity every 2 h until 24 h, and at 36 h and 48 h (data not shown). We determined appropriate assay time points as 6 h (STS or H_2O_2), 24 h (TG or MG132) and 48 h (ETP). Cell viability was significantly reduced (Fig. 1, left panels) and caspase-3/7 activity relative to the baseline activities was significantly increased (Fig. 1, right panels) in mutant PS1-transfected cells compared to wild-type PS1-transfected cells after treatments with STS (Fig. 1A), TG (Fig. 1C), MG132 (Fig. 1D), and H_2O_2 (Fig. 1E). Similar effects were observed after treatment with ETP, although the differences did not reach statistical significance (Fig. 1B).

Baseline activities of caspase-4, -8, and -9 are increased in mutant PS1-transfected cells

Next, to investigate whether the PS1 mutants accelerates the activation of upstream initiator caspases, we measured the specific activities of caspase-4 relative to ER stress, caspase-8 relative to the Fas-receptor-mediated pathway, and caspase-9 relative to mitochondrial damage. The baseline activity levels of caspase-4, -8 and -9 were significantly elevated in mutant PS1-transfected cells compared to wild-type PS1-transfected cells (Fig. 2A-C, left panels). Before measuring the caspase activities after treatment with toxic agents, we checked the effects of DMSO on the caspase activities, since DMSO was used as the solvent for these toxic agents with the exception of H_2O_2. A final concentration of 0.1% DMSO was added to the medium with the agents in the following assays.

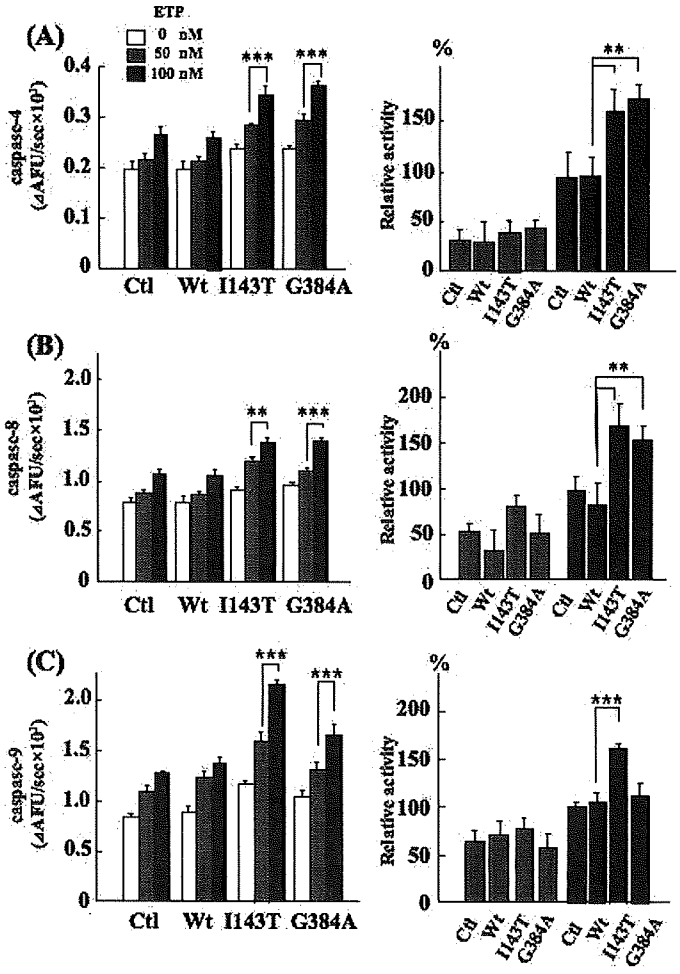

Fig. 4. Activities of caspase-4, -8 and -9 in control (Ctl), wild-type PS1-transfected (Wt) and mutant PS1-transfected (I143T or G384A) cells after treatment with ETP for 48 h. (A) Caspase-4 activity. (B) Caspase-8 activity. (C) Caspase-9 activity. The left panels show the individual activities, while the right panels show the relative activities to the activities in control cells treated with 100 nM ETP. $^{**}p < 0.001$; $^{***}p < 0.0001$.

Caspase-8 activity was diminished by 0.1% DMSO, whereas caspase-4 and -9 activities seemed to be unaffected (Fig. 2A-C, right panels), indicating that the effect of DMSO needed to be taken into account during evaluation of caspase-8 activity.

Activities of caspase-4, -8, and -9 after treatment with apoptotic agents are variably elevated in mutant PS1-transfected cells

Next, we examined the changes in the caspase-4, -8 and -9 activities in the proapoptosis process induced by various toxic agents. After a 6-h treatment with STS, caspase-4 activity was significantly elevated at 50 nM in all cell types (Fig. 3A, left) while caspase-8 (Fig. 3B, left) and caspase-9 (Fig. 3C, left) activities were significantly elevated only in mutant PS1-transfected cells. To further assess the effects of the PS1 mutants on the activation of these caspases, we compared the relative activation levels of the caspases in different cell types. Caspase-4 was activated in mutant PS1-transfected cells ~1.5-fold more than in wild-type PS1-transfected cells (Fig. 3A, right). Increases in caspase-8 and -9 activities were less prominent than increases in caspase-4 activity, and the relative activation was more remarkable in I143T-mutant PS1-transfected cells than in G384A-mutant PS1-transfected cells (Fig. 3B and C, right). After a 48-h treatment with ETP, ~1.5-fold increases in the activities of caspase-4, -8 and -9 were observed in all cell types (Fig. 4A-C, left). In comparisons of the relative activities, caspase-4 and -8 activation levels were higher in mutant PS1-transfected

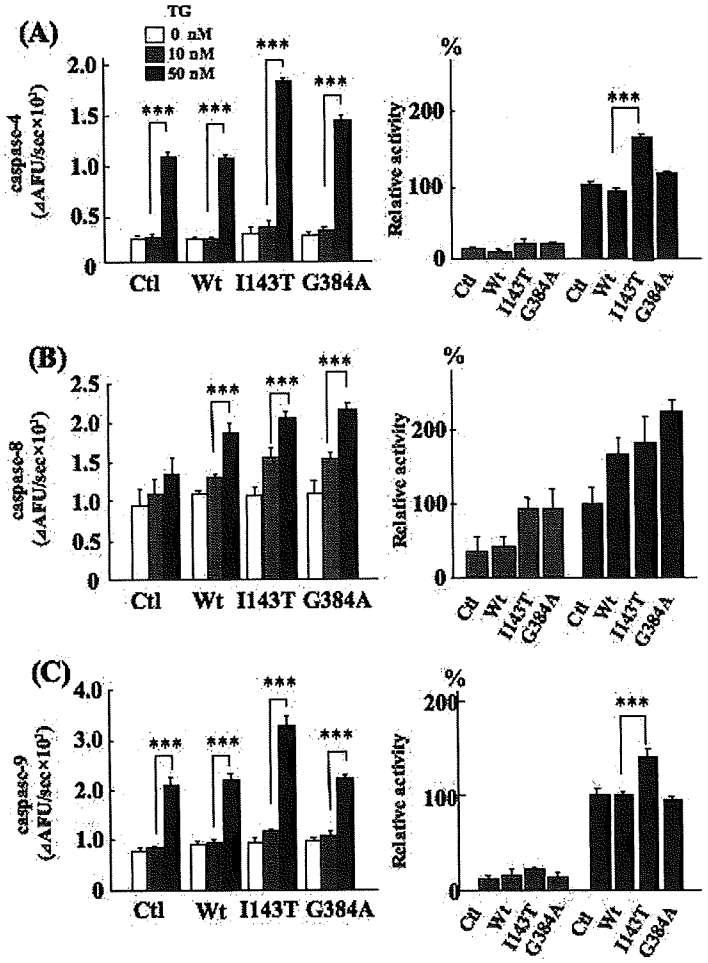

Fig. 5. Activities of caspase-4, -8 and -9 in control (Ctl), wild-type PS1-transfected (Wt) and mutant PS1-transfected (I143T or G384A) cells after treatment with TG for 24 h. (A) Caspase-4 activity. (B) Caspase-8 activity. (C) Caspase-9 activity. The left panels show the individual activities, while the right panels show the relative activities to the activities in control cells treated with 50 nM TG. $^{**}p < 0.001$; $^{***}p < 0.0001$.

cells than in wild-type PS1-transfected cells (Fig. 4A and B, right), while caspase-9 activation was significantly increased only in I143T-mutant PS1-transfected cells (Fig. 4C, right). After a 24-h treatment with 50 nM TG, 3 to 4-fold elevation of caspase-4 and -9 activities was observed (Fig. 5A and C, left) with ~2-fold elevation of caspase-8 activity in wild-type and mutant PS1-transfected cells (Fig. 5B, left). In comparisons of relative activities, caspase-4 and -9 activity levels were significantly elevated only in I143T-mutant PS1-transfected cells compared to wild-type PS1-transfected cells (Fig. 5A and C, right). No significant differences were found for caspase-8 activity (Fig. 5B, right). After a 24-h treatment with another ER-stress inducer, tunicamycin, similar effects were observed (data not shown). After a 24-h treatment with 0.3 nM MG132, remarkable elevations of caspases-4 and -9 activities were observed in all cell types (Fig. 6A and C, left) with gradual elevation of caspase-8 activity (Fig. 6B, left). In comparisons of the relative activities, caspase-4 and -8 activities were accelerated in mutant PS1-transfected cells (Fig. 6A and B, right), while caspase-9 was ~1.5-fold more activated only in I143T-mutant PS1-transfected cells (Fig. 6C, right). After a 6-h treatment with H_2O_2, remarkable elevations of caspase-4 and -9 activities were observed in all cell types (Fig. 7A and C, left), while elevation of caspase-8 activity was only slight (Fig. 7B, left). In comparisons of the relative activities, it was of interest that significantly higher activation levels of caspase-4, -8 and -9 were detected in G384A-mutant PS1-transfected cells but not in I143T-mutant PS1-transfected cells (Fig. 7A-C, right). All these results of caspase-4, -8 and -9 activations are summarized in Table 1.

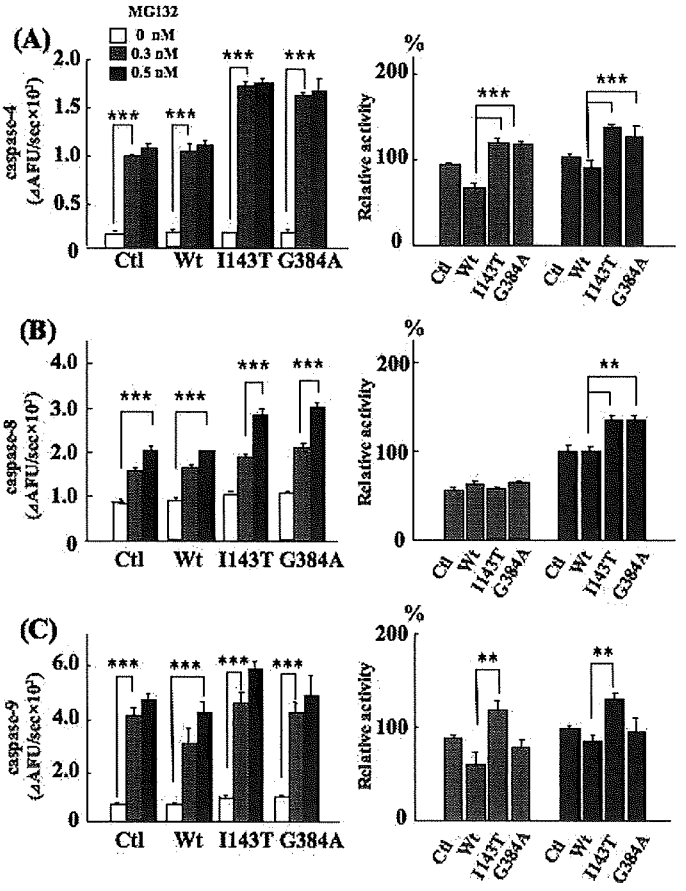

Fig. 6. Activities of caspase-4, -8 and -9 in control (Ctl), wild-type PS1-transfected (Wt) and mutant PS1-transfected (I143T or G384A) cells after treatment with MG132 for 24 h. (A) Caspase-4 activity. (B) Caspase-8 activity. (C) Caspase-9 activity. The left panels show the individual activities, while the right panels show the relative activities to the activities in control cells treated with 0.5 nM MG132. $^{**}p < 0.001$; $^{***}p < 0.0001$.

Table 1
Activation of caspase-4, -8 and -9

	I143T			G384A		
	cas-4	cas-8	cas-9	cas-4	cas-8	cas-9
STS	↑	↑	↑	↑	→	→
ETP	↑	↑	↑	↑	↑	→
TG	↑	→	↑	→	→	→
MG132	↑	↑	↑	↑	↑	→
H_2O_2	→	→	→	↑	↑	↑

GRP78, Bid, and Bax are induced by STS, TG, and H_2O_2

To confirm apoptosis induction by these agents in a different method, we analyzed some apoptosis markers. 78-kD GRP78 [29], 15-kD truncated Bid [30] and 21-kD Bax [31] proteins are known to be associated with ER stress, FAS signal, and mitochondrial impairment, respectively. Western blot analysis revealed that STS, TG and H_2O_2 treatments all upregulated expression of GRP78, truncated Bid and Bax proteins (Fig. 8). Induction of GRP78 or Bax was remarkable in treatment with TG or STS, respectively, which may be consistent with the target of each agent. Treatment with STS or TG, but not H_2O_2, increased Bax expression in I143T-mutant PS1-transfected cells more apparently compared to G384A-mutant PS1-transfected cells. Also, H_2O_2 treatment increased truncated Bid, which is generated by caspase-8 [30], in G384A-mutant PS1-transfected cells. Therefore, such variation may correspond, at least in part, to variation of caspase-4, -8 and -9 activation in these two mutant PS1-transfected cells (Table 1).

BACE and γ-secretase inhibitors attenuate caspase-3/7 upregulation and apoptosis

Since *PS1* gene mutations are well known to increase $A\beta_{42}$ generation, it is an important issue whether the

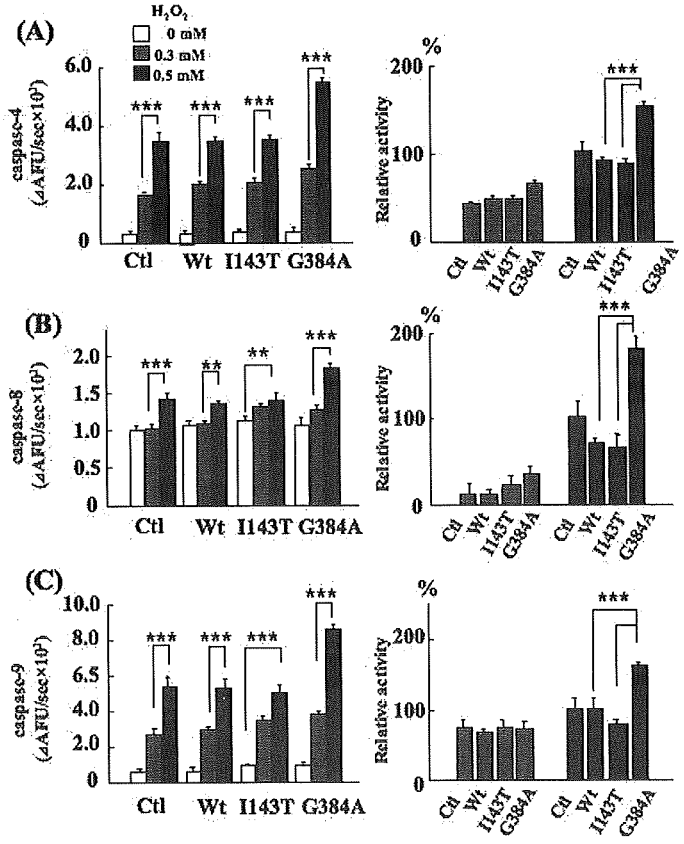

Fig. 7. Activities of caspase-4, -8 and -9 in control (Ctl), wild-type PS1-transfected (Wt) and mutant PS1-transfected (I143T or G384A) cells after treatment with H_2O_2 for 6 h. (A) Caspase-4 activity. (B) Caspase-8 activity. (C) Caspase-9 activity. The left panels show the individual activities, while the right panels show the relative activities to the activities in control cells treated with 0.5 mM H_2O_2. $^{**}p < 0.001$; $^{***}p < 0.0001$.

apoptosis-promoting effects of PS1 mutants are mediated by $A\beta_{42}$ overproduction. $A\beta$ is generated from $A\beta$PP through proteolytic cleavage by BACE and γ-secretase, and inhibitors of these enzymes inhibit $A\beta$ generation. We examined the effects of BACE or γ-secretase inhibitors on cell viability and caspase-3/7 activity after treatment with apoptosis-inducing agents. Inhibition of $A\beta$ generation using these secretase inhibitors was confirmed in our other report [26], and these secretase inhibitors did not alter baseline caspase-3/7 activity and cell viability (data not shown). Treatment of mutant PS1-transfected cells with the BACE inhibitor recovered cell viability in part (Fig. 9A-C, left) and counteracted caspase-3/7 activation (Fig. 9A-C, right) significantly against treatment with STS (9A), TG (9B), and H_2O_2 (9C). Similarly, treatment with the γ-secretase inhibitor recovered cell viability in part (Fig. 10A-C, left) and significantly counteracted caspase-3/7 activation (Fig. 10A-C, right). After treatment with ETP or MG132, similar but not significant effects were observed (data not shown). In addition, we examined effects of BACE or γ-secretase inhibitors on initiator caspases, and found that elevation of baseline caspase-4 and -9 activity in mutant PS1-transfected cells and caspase-9 upregulation after treatment with H_2O_2 in G384A-mutant PS1-transfected cells were not counteracted (data not shown).

DISCUSSION

Synaptic damage related to extracellular $A\beta$ oligomers [3] and intraneuronal $A\beta$ [32] may contribute to cognitive dysfunction in an early stage of AD, while numerous neuronal cell losses may occur in late stage AD. Since *PS1* gene mutations-related FAD cause early-onset dementia, neuronal cell death may be accelerated in FAD with PS1 mutants more remarkably than in sporadic AD. PS1 is involved in inhibition of apoptosis via the SAPK/JNK pathway by interacting with

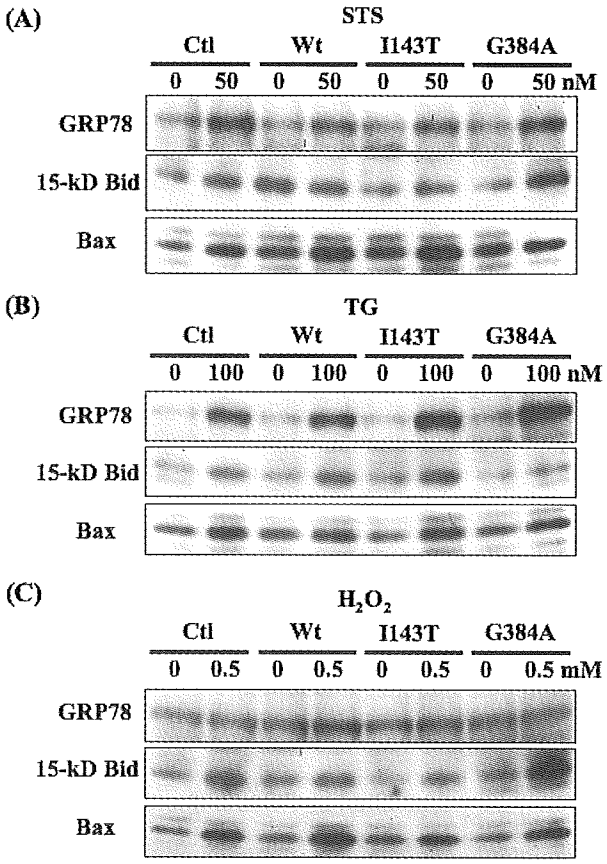

Fig. 8. Western blot analysis of GRP78 (78 kD), truncated Bid (15 kD) and Bax (21 kD) in control (Ctl), wild-type PS1-transfected (Wt), I143T-mutant PS1-transfected (I143T) or G384A-mutant PS1-transfected cells after treatment with STS (A), TG (B) or H_2O_2 (C) for 24 h.

QM/Jif-1, a negative regulator of c-jun [33], and interacts with apoptosis-regulating proteins, Bcl-X_L [34], Bcl-2 [35], Omi [36], and presenilin associated protein (PSAP) [37]. Mutant PS1 affects β-catenin function [38], which may impair Wnt signaling resulting in loss of anti-apoptosis effect [39]. Moreover, Aph-1 and Pen-2 have anti-apoptotic functions when forming the γ-secretase complex with wild-type PS1, although enzymatic activity is not required [40]. Since many of these proteins are associated with the mitochondrial or ER stress pathways, elevation of caspase-4 and -9 activity by the mutant PS1 may be related to these proteins.

STS is generally known to cause change of mitochondrial membrane permeability, release of cytochrome C oxidase, and activation of caspase-9. Although STS treatment elevated caspase-4 activity remarkably in the present study, a previous report revealed that STS could stimulate caspase-4 activity [41]. Considerable increases in caspase-9 activity were observed after treatments with TG, an ER stress inducer. Caspase-9 may be activated by ER stress through concomitant activation of the mitochondrial apoptosis pathway mediated by p53, PUMA, and NOXA [42–44]. Also, proteasome inhibition by MG132 may induce apoptosis through the mitochondrial pathway [45], caspase-8-related apoptosis [46], and ER stress [47]. Thus, these agents may activate multiple initiator caspases. Patterns of caspase activation by treatment with STS, ETP and MG132 were basically similar (Table 1). Caspase-4 was upregulated in both types of mutant PS1-transfected cells, caspase-9 was upregulated in I143T-mutant PS1-transfected cells but not in G384A-mutant transfected cells, and caspase-8 activity was variable. Caspase-8 activity may have been perturbed by the presence of 0.1% DMSO. In contrast, TG induced activation of caspase-4 and -8 in I143T-mutant PS1-transfected cells, while H_2O_2 induced activation of caspase-4, -8 and -9 in G384A-mutant PS1-transfected cells, indicating that some common and different pathways of apoptosis may be variably accel-

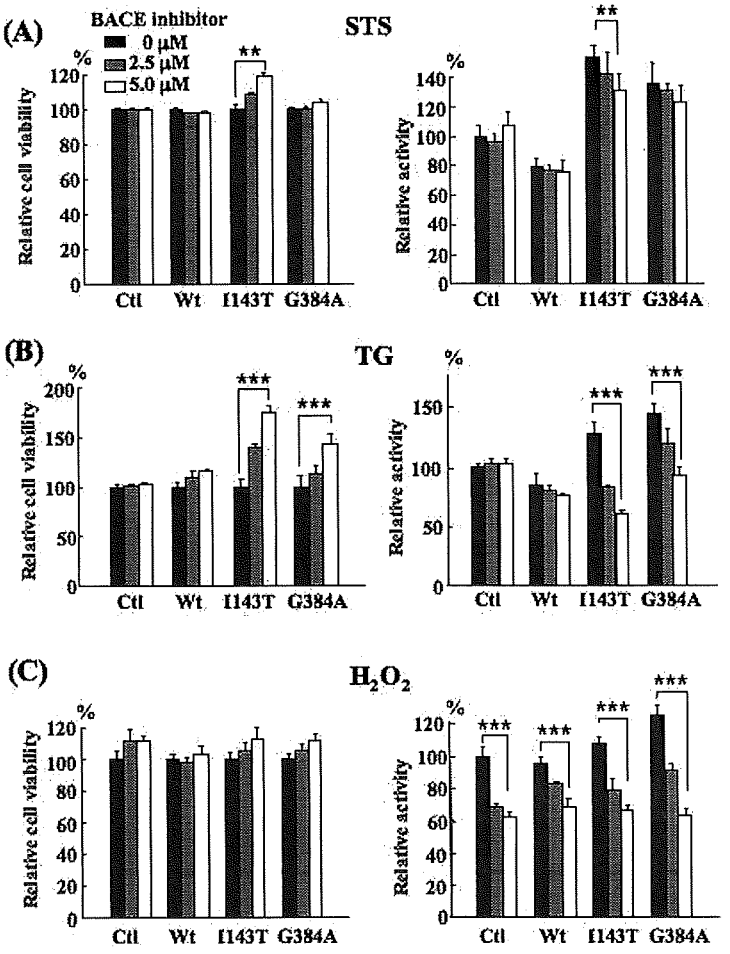

Fig. 9. Effects of BACE inhibitor on cell viability (left) and caspase-3/7 activity (right) in cells treated with 50 nM STS for 6 h (A), 50 nM TG for 24 h (B), and 0.7 mM H_2O_2 for 6 h (C). $^{**}p < 0.001$; $^{***}p < 0.0001$.

erated in I143T-mutant PS1-transfected and G384A-mutant PS1-transfected cells.

We demonstrated that decreased cell viability and increased caspase-3/7 activity were counteracted in part by treatment with BACE or γ-secretase inhibitors. One of the mechanisms may be inhibition of AICD-related p53 mRNA overexpression [48]. Alternatively, intracellular Aβ_{42} itself may contribute to p53 mRNA overexpression [49,50]. As we demonstrated in our other report [26], p53 protein levels were increased and treatment with BACE or γ-secretase inhibitors attenuated p53 protein accumulation in both PS1 mutants. Thus, inhibition of Aβ generation-related proteasomal dysfunction and p53 protein accumulation may be a common mechanism to recover cell viability and to attenuate caspase-3/7 activity in these mutant PS1-transfected cells. However, the mechanism of differential upregulation of initiator caspases, especially caspase-9, in these mutant PS1-transfected cells is unclear. Since both secretase inhibitors did not counteract elevation of initiator caspases activity significantly (data not shown), Aβ-unrelated mechanisms might underlie the effects of these PS1 mutants. Thus, each PS1 gene mutation may upregulate both Aβ-related and -unrelated apoptotic process. Since we found proteasome inhibition associated with intracellular Aβ in mutant PS1-transfected cells [26], Aβ and proteasome might be involved in the caspase-3/7 activation process.

G384A-mutant PS1-transfected cells generate higher levels of Aβ_{42} than I143T-mutant PS1-transfected cells [24]. G384A is located close to the γ-secretase enzymatic activity site of PS1, whereas I143T is located in the N-terminus of PS1 [51], which may be a reason for different Aβ levels in PS1 mutants. While, a recent report showed that G384A-mutant PS1 increased Aβ_{42}/Aβ_{40} secretion ratio by decreasing Aβ_{40} secre-

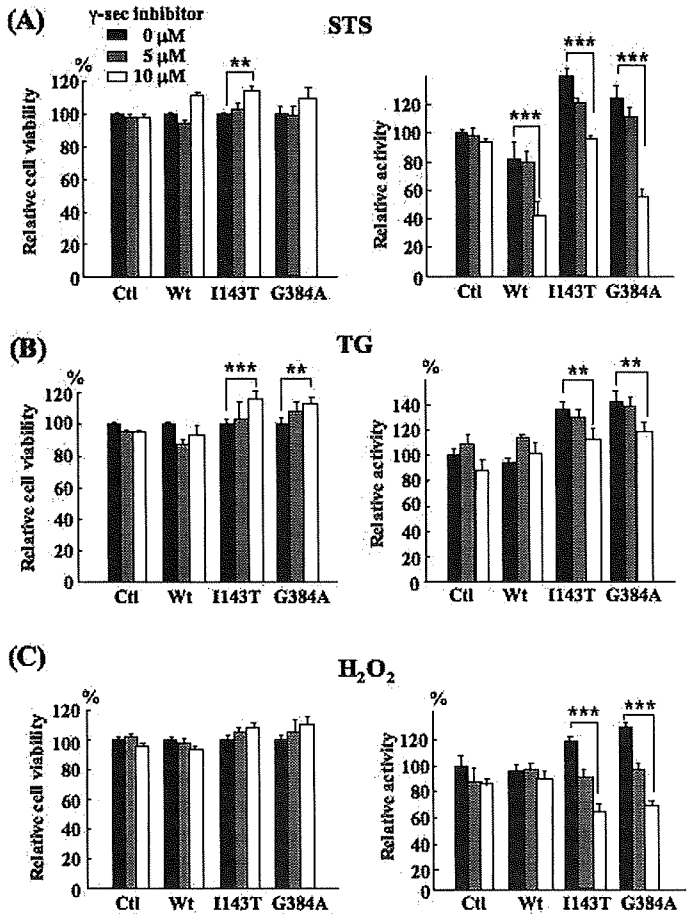

Fig. 10. Effects of γ-secretase inhibitor on cell viability (left) and caspase-3/7 activity (right) in cells treated with 50 nM STS for 6 h (A), 50 nM TG for 24 h (B), and 0.7 mM H_2O_2 for 6 h (C). $^{**}p < 0.001$; $^{***}p < 0.0001$.

tion in PS1-knockin fibroblasts [52], which might be due to a shift from secretion to intracellular accumulation of Aβ. While, a recent report suggested that FAD-related *PS1* gene mutations, including G384A, disrupt the calcium leak function of PS1, whereas fronto-temporal dementia (FTD)-associated mutations do not [53]. Since over 100 mutations of the *PS1* gene are known in FAD [51], the pathogeneses of PS1 mutants may be highly variable among the mutations. It is necessary to understand common pathogenesis and each mutation-associated pathogenesis of PS1, and such investigation may be useful for development of drugs to prevent neuronal apoptosis in FAD.

ACKNOWLEDGMENTS

This work was supported by a Grant-in-Aid for Scientific Research from the Japanese Ministry of Education, Science, Sports and Culture and by Health and Labour Sciences Research Grant from the Japanese Ministry of Health, Labour and Welfare (H15-Kokoro-001).

REFERENCES

[1] Hardy J, Selkoe DJ (2002) The amyloid hypothesis of Alzheimer's disease: progress and problems on the road to therapeutics. *Science* **297**, 353-356.
[2] Younkin SG (1995) Evidence that Aβ42 is the real culprit in Alzheimer's disease. *Ann Neurol* **37**, 287-288.
[3] Walsh DM, Klyubin I, Fadeeva JV, Rowen MJ, Selkoe DJ (2002) Amyloid-β oligomers: their production, toxicity and therapeutic inhibition. *Biochem Soc Trans* **30**, 552-557.
[4] Lesné S, Koh MT, Kotilinek L, Kayed R, Glabe CG, Yang A, Gallagher M, Ashe KH (2006) A specific amyloid-β protein assembly in the brain impairs memory. *Nature* **440**, 352-357.
[5] Rocchi A, Pellegrini S, Siciliano G, Murri L (2003) Causative and susceptibility genes for Alzheimer's disease: a review. *Brain Res Bull* **61**,1-24.

[6] Zhang J, Kang DE, Xia W, Okochi M, Mori H, Selkoe DJ, Koo EH (1998) Subcellular distribution and turnover of presenilins in transfected cells. *J Biol Chem* **273**, 12436-12442.
[7] Pasternak SH, Bagshaw RD, Guiral M, Zhang S, Ackerley CA, Pak BJ, Callahan JW, Mahuran DJ (2003) Presenilin-1, nicastrin, amyloid precursor protein, and γ-secretase activity are co-localized in the lysosomal membrane. *J Biol Chem* **278**, 26687-26694.
[8] Vetrivel KS, Cheng H, Lin W, Sakurai T, Li T, Nukina N, Wong PC, Xu H, Thinakaran G (2004) Association of γ-secretase with lipid rafts in post-Golgi and endosome membranes. *J Biol Chem* **279**, 44945-44954.
[9] Uemura K, Kuzuya A, Shimozono Y, Aoyagi N, Ando K, Shimohama S, Kinoshita A (2007) GSK3β activity modifies the localization and function of presenilin 1. *J Biol Chem* **282**, 15823-15832.
[10] Hansson CA, Frykman S, Farmery MR, Tjernberg LO, Nilsberth C, Pursglove SE, Ito A, Winblad B, Cowburn RF, Thyberg J, Ankarcrona M (2004) Nicastrin, presenilin, APH-1, and PEN-2 form active γ-secretase complexes in mitochondria. *J Biol Chem* **279**, 51654-51660.
[11] Kaether C, Haass C, Steiner H (2006) Assembly, trafficking and function of γ-secretase. *Neurodegener Dis* **3**, 275-283.
[12] Kopan R, Ilagan MX (2004) γ-secretase: proteasome of the membrane? *Nat Rev Mol Cell Biol* **5**, 499-504.
[13] Raemaekers T, Esselens C, Annaert W (2005) Presenilin 1: more than just γ-secretase. *Biochem Soc Trans* **33**, 559-562.
[14] Selkoe DJ (2001) Alzheimer's disease: genes, proteins, and therapy. *Physiol Rev* **81**, 741-766.
[15] Katayama T, Imaizumi K, Manabe T, Hitomi J, Kudo T, Tohyama M (2004) Induction of neuronal death by ER stress in Alzheimer's disease. *J Chem Neuroanat* **28**, 67-78.
[16] Thinakaran G, Sisodia SS (2006) Presenilins and Alzheimer disease: the calcium conspiracy. *Nat Neurosci* **9**, 1354-1355.
[17] McCarthy JV (2005) Involvement of presenilins in cell-survival signalling pathways. *Biochem Soc Trans* **33**, 568-572.
[18] LeBlanc AC (2005) The role of apoptotic pathways in Alzheimer's disease neurodegeneration and cell death. *Curr Alzheimer Res* **2**, 389-402.
[19] Ferri KF, Kroemer G (2001) Organelle-specific initiation of cell death pathways. *Nat Cell Biol* **3**, E255-E263.
[20] Cruts M, Backhovens H, Wang SY, Van Gassen G, Theuns J, De Jonghe CD, Wehnert A, De Voecht J, De Winter G, Cras P, Bruyland M, Datson N, Weissenbach J, Dunnen JT, Martin JJ, Hendriks L, Van Broeckhoven C (1995) Molecular genetic analysis of familial early-onset Alzheimer's disease linked to chromosome 14q24.3. *Hum Mol Genet* **4**, 2363-2371.
[21] Vanderhoeven I, Cras P, Martin JJ, Van Broeckhoven C, De Jonghe C (1999) Proteolytic processing of presenilin-1 in human lymphoblasts is not affected by the presence of the I143T and G384A mutations. *Neurosci Lett* **274**,183-186.
[22] Van Gassen G, De Jonghe C, Nishimura M, Yu G, Kuhn S, St George-Hyslop P, Van Broeckhoven C (2000) Evidence that the β-catenin nuclear translocation assay allows for measuring presenilin 1 dysfunction. *Mol Med* **6**, 570-580.
[23] Hamano T, Muto T, Tabira T, Araki W, Kuriyama M, Mihara T, Yano S, Yamamoto H (2005) Abnormal intracellular trafficking of high affinity nerve growth factor receptor, Trk, in stable transfectants expressing presenilin 1 protein. *Brain Res Mol Brain Res* **137**, 70-76.
[24] De Jonghe C, Cras P, Vanderstichele H, Cruts M, Vanderhoeven I, Smouts I, Vanmechelen E, Martin JJ, Hendriks L, Van Broeckhoven C (1999) Evidence that Aβ42 plasma levels in presenilin-1 mutation carriers do not allow for prediction of their clinical phenotype. *Neurobiol Dis* **6**, 280-287.
[25] Shirotani K, Takahashi K, Tabira T (1999) Effects of presenilin N-terminal fragments on production of amyloid β peptide and accumulation of endogenous presenilins. *Neurosci Lett* **262**, 37-40.
[26] Ma L, Ohyagi Y, Miyoshi K, Sakae N, Motomura K, Taniwaki T, Furuya H, Takeda K, Tabira T, Kira J (2009) Increase in p53 protein levels by presenilin 1 gene mutations and its inhibition by secretase inhibitors. *J Alzheimers Dis* **16**, 565-575.
[27] Capell A, Meyn L, Fluhrer R, Teplow DB, Walter J, Haass C (2002) Apical sorting of β-secretase limits amyloid β-peptide production. *J Biol Chem* **277**, 5637-5643.
[28] Shearman MS, Beher D, Clarke EE, Lewis HD, Harrison T, Hunt P, Nadin A, Smith AL, Stevenson G, Castro JL (2000) L-685458, an aspartyl protease transition state mimic, is a potent inhibitor of amyloid β-protein precursor γ-secretase activity. *Biochemistry* **39**, 8698-8704.
[29] Ni M, Lee AS (2007) ER chaperones in mammalian development and human diseases. *FEBS Lett* **581**, 3641-3651.
[30] Li H, Zhu H, Xu C-J, Yuan J (1998) Cleavage of BID by caspase 8 mediates the mitochondrial damage in the Fas pathway of apoptosis. *Cell* **94**, 491-501.
[31] Zinkel S, Gross A, YangE (2006) BCL2 family in DNA damage and cell cycle control. *Cell Death Differ* **13**, 1351-1359.
[32] Takahashi RH, Milner TA, Li F, Nam EE, Edgar MA, Yamaguchi H, Beal MF, Xu H, Greengard P, Gouras GK (2002) Intraneuronal Alzheimer Aβ42 accumulates in multivesicular bodies and is associated with synaptic pathology. *Am J Pathol* **161**, 1869-1879.
[33] Imafuku I, Masaki T, Waragai M, Takeuchi S, Kawabata M, Hirai S, Ohno S, Nee LE, Lippa CF, Kanazawa I, Imagawa M, Okazawa H (1999) Presenilin 1 suppresses the function of c-Jun homodimers via interaction with QM/Jif-1. *J Cell Biol* **147**, 121-134.
[34] Passer BJ, Pellegrini L, Vito P, Ganjei JK, D'Adamio L (1999) Interaction of Alzheimer's presenilin-1 and presenilin-2 with Bcl-X(L): a potential role in modulating the threshold of cell death. *J Biol Chem* **274**, 24007-24013.
[35] Alberici A, Moratto D, Benussi L, Gasparini L, Ghidoni R, Gatta LB, Finazzi D, Frisoni GB, Trabucchi M, Growdon JH, Nitsch RM, Binetti G (1999) Presenilin 1 protein directly interacts with Bcl-2. *J Biol Chem* **274**, 30764-30769.
[36] Gupta S, Singh R, Datta P, Zhang Z, Orr C, Lu Z, Dubois G, Zervos AS, Meisler MH, Srinivasula SM, Fernandes-Alnemri T, Alnemri ES (2004) The C-terminal tail of presenilin regulates Omi/HtrA2 protease activity. *J Biol Chem* **279**, 45844-45854.
[37] Xu X, Shi YC, Gao W, Mao G, Zhao G, Agrawal S, Chisolm GM, Sui D, Cui MZ (2002) The novel presenilin-1-associated protein is a proapoptotic mitochondrial protein. *J Biol Chem* **277**, 48913-48922.
[38] Killick R, Pollard CC, Asuni AA, Mudher AK, Richardson JC, Rupniak HT, Sheppard PW, Varndell IM, Brion JP, Levey AI, Levy OA, Vestling M, Cowburn R, Lovestone S, Anderton BH (2001) Presenilin 1 independently regulates β-catenin stability and transcriptional activity. *J Biol Chem* **276**, 48554-48561.
[39] You Z, Saims D, Chen S, Zhang Z, Guttridge DC, Guan KL, MacDougald OA, Brown AM, Evan G, Kitajewski J, Wang CY (2002) Wnt signaling promotes oncogenic transformation by inhibiting c-Myc-induced apoptosis. *J Cell Biol* **157**, 429-440.
[40] Dunys J, Kawarai T, Sevalle J, Dolcini V, St George-Hyslop P, Alves da Costa C, Checler F (2007) p53-dependent Aph-1 and Pen-2 anti-apoptotic phenotype requires the integrity of

the γ-secretase complex but is independent of its activity. *J Biol Chem* **282**, 10516-10525.

[41] Cusinato F, Pighin I, Luciani S, Trevisi L (2006) Synergism between staurosporine and drugs inducing endoplasmic reticulum stress. *Biochem Pharmacol* **71**, 1562-1569.

[42] Li J, Lee B, Lee AS (2006) Endoplasmic reticulum stress-induced apoptosis: multiple pathways and activation of p53-up-regulated modulator of apoptosis (PUMA) and NOXA by p53. *J Biol Chem* **281**, 7260-7270.

[43] Reimertz C, Kogel D, Rami A, Chittenden T, Prehn JH (2003) Gene expression during ER stress-induced apoptosis in neurons: induction of the BH3-only protein Bbc3/PUMA and activation of the mitochondrial apoptosis pathway. *J Cell Biol* **162**, 587-597.

[44] Tashiro J, Kikuchi S, Shinpo K, Kishimoto R, Tsuji S, Sasaki H (2007) Role of p53 in neurotoxicity induced by the endoplasmic reticulum stress agent tunicamycin in organotypic slice cultures of rat spinal cord. *J Neurosci Res* **85**, 395-401.

[45] Lang-Rollin I, Maniati M, Jabado O, Vekrellis K, Papantonis S, Rideout HJ, Stefanis L (2005) Apoptosis and the conformational change of Bax induced by proteasomal inhibition of PC12 cells are inhibited by bcl-xL and bcl-2. *Apoptosis* **10**, 809-820.

[46] Hougardy BM, Maduro JH, Van der Zee AG, De Groot DJ, Van den Heuvel FA, De Vries EG, De Jong S (2006) Proteasome inhibitor MG132 sensitizes HPV-positive human cervical cancer cells to rhTRAIL-induced apoptosis. *Int J Cancer* **118**, 1892-1900.

[47] Obeng EA, Carlson LM, Gutman DM, Harrington Jr WJ, Lee KP and Boise LH (2006) Proteasome inhibitors induce a terminal unfolded protein response in multiple myeloma cells. *Blood* **107**, 4907-4916.

[48] Alves da Costa C, Sunyach C, Pardossi-Piquard R, Sevalle J, Vincent B, Boyer N, Kawarai T, Girardot N, St George-Hyslop P, Checler F (2006) Presenilin-dependent γ-secretase-mediated control of p53-associated cell death in Alzheimer's disease. *J Neurosci* **26**, 6377-6385.

[49] Ohyagi Y, Asahara H, Chui DH, Tsuruta Y, Sakae N, Miyoshi K, Yamada T, Kikuchi H, Taniwaki T, Murai H, Ikezoe K, Furuya H, Kawarabayashi T, Shoji M, Checler F, Iwaki T, Makifuchi T, Takeda K, Kira J, Tabira T (2005) Intracellular Aβ42 activates p53 promoter: a pathway to neurodegeneration in Alzheimer's disease. *FASEB J* **19**, 255-257.

[50] Ohyagi Y, Tabira T (2006) Intracellular amyloid β-protein and its associated molecules in the pathogenesis of Alzheimer's disease. *Mini Rev Med Chem* **6**, 1075-1080.

[51] Tandon A, Fraser P (2002) The presenilins. *Genome Biol* **3**, reviews 3014.1-3014.9.

[52] Shimojo M, Sahara N, Murayama M, Ichinose H, Takashima A (2007) Decreased Aβ secretion by cells expressing familial Alzheimer's disease-linked mutant presenilin 1. *Neurosci Res* **57**, 446-453.

[53] Nelson O, Tu H, Lei T, Bentahir M, De Strooper B, Bezprozvanny I (2007) Familial Alzheimer disease-linked mutations specifically disrupt Ca^{2+} leak function of presenilin 1. *J Clin Invest* **117**, 1230-1239.

Journal of Alzheimer's Disease 16 (2009) 565–575
DOI 10.3233/JAD-2009-0990
IOS Press

Increase in p53 Protein Levels by *Presenilin 1* Gene Mutations and its Inhibition by Secretase Inhibitors

Linqing Ma[a], Yasumasa Ohyagi[a,*], Katsue Miyoshi[a], Nobutaka Sakae[a], Kyoko Motomura[a], Takayuki Taniwaki[a], Hirokazu Furuya[b], Kazuya Takeda[c], Takeshi Tabira[c] and Jun-ichi Kira[a]
[a]*Department of Neurology, Neurological Institute, Graduate School of Medical Sciences, Kyushu University, Fukuoka, Japan*
[b]*Clinical Research Center, National Omuta Hospital, Omuta, Fukuoka, Japan*
[c]*National Institute for Longevity Sciences, NCGG, Obu, Aichi, Japan*

Abstract. *Presenilin 1* (*PS1*) gene mutations are the major causes of early-onset familial Alzheimer's disease and are known to increase amyloid-β_{42} ($A\beta_{42}$) production as well as to promote apoptosis. We have recently reported that intracellular $A\beta_{42}$ activates p53 mRNA expression and promotes p53-dependent apoptosis. Here, we examined the p53 mRNA and protein levels in cells transfected with wild-type and I143T/G384A mutant *PS1* genes. Although the baseline p53 mRNA levels remained unaltered, the p53 protein levels were significantly elevated in mutant PS1-transfected cells. Treatments with apoptosis-inducing agents induced significant elevation of the p53 protein but not p53 mRNA levels in mutant PS1-transfected cells. Treatment with a β-secretase inhibitor and γ-secretase inhibitor decreased the intracellular $A\beta$ levels in amyloid-β protein precursor ($A\beta$PP) and PS1-double transfected cells, and restrained upregulation of the p53 protein levels in the mutant PS1-transfected cells. Also, we found that proteasome activity was decreased in mutant PS1-transfected cells compared to wild-type PS1-transfected cells. Proteasome activity was further decreased in $A\beta$PP/PS1-double transfected cells. Taken together, p53-dependent apoptosis upregulated by the I143T/G384A mutant *PS1* gene may be associated, at least in part, with intracellular $A\beta$ and proteasome impairment.

Keywords: Alzheimer's disease, p53, presenilin, proteasome, β-secretase, γ-secretase

INTRODUCTION

Alzheimer's disease (AD) is the most common dementia in elderly people and is pathologically characterized by intracellular neurofibrillary tangle formation, extracellular amyloid-β protein ($A\beta$) deposition, and global loss of neurons in the brain. A widely known hypothesis for AD pathogenesis, designated the amyloid cascade theory, suggests that extracellular $A\beta$ ending at amino acid 42 ($A\beta_{42}$), a major aggregative species, forms neurotoxic oligomers [1]. Therefore, inhibition of $A\beta_{42}$ generation and removal of extracellular $A\beta_{42}$ are thought to be therapeutic targets for AD [2]. However, some pathological studies have demonstrated that $A\beta_{42}$ accumulates in neurons before senile plaque formation in AD [3,4] and Down syndrome [5,6]. $A\beta_{42}$ was also reported to accumulate in neurons in several familial AD (FAD) mouse models [7–10], and we found $A\beta_{42}$ accumulation to be associated with neuronal apoptosis *in vitro* [11] and in AD brain [12]. In addition, it was reported that intraneuronal $A\beta_{42}$ induces neuronal apoptosis in a dose-dependent manner [13–15]. Thus, intracellular $A\beta_{42}$ accumulation may be tightly linked to neuronal apoptosis and AD pathology.

*Corresponding author: Yasumasa Ohyagi, MD, 3-1-1 Maidashi, Higashi-ku, Fukuoka 812-8582, Japan. Fax: +81 92 642 5352; E-mail: ohyagi@neuro.med.kyushu-u.ac.jp.

ISSN 1387-2877/09/$17.00

Early-onset FAD is an autosomal dominant disorder that co-seggregates with the genes for presenilin (PS) 1, PS2, and amyloid-β protein precursor (AβPP) [16]. The pathogenesis of these gene mutations has been suggested to be multiple. First, PS proteins form parts of the γ-secretase complex that produces Aβ from AβPP, and mutations in the *PS1* and *PS2* genes enhance selective Aβ_{42} generation [17]. Second, mutant PS1 and PS2 proteins accelerate apoptosis via various pathways [18–20]. Recently, we have demonstrated that cytosolic Aβ_{42} may be transferred to the nucleus by Aβ-related death-inducing protein (AB-DIP) [21] and may promote p53 mRNA expression and apoptosis [22,23]. Moreover, it has been reported that amyloid intracellular C-terminal domain C59 (AICDC59), which is produced by γ-secretase, also activates p53 mRNA expression [24]. Thus, abnormally increased γ-secretase activity and p53 expression may be involved in the neurodegeneration associated with FAD-related *PS1* gene mutations. P53 is a transcriptional factor that regulates apoptosis [25], and its expression is regulated by the ubiquitin-proteasome system (UPS) at the protein level and by transcriptional factors at the mRNA level [26,27]. We found accelerating effects of I143T and G384A PS1 mutants on the activation of caspases in our other report [28]. Here, we examined the p53 mRNA and protein levels in cells transfected with wild-type PS1 or PS1 mutants.

MATERIALS AND METHODS

Cell culture, apoptosis-inducing agents and β-/γ-secretase inhibitors

Human wild-type, I143T-mutant and G384A-mutant PS1 cDNAs were subcloned into the pCEP4 vector (Invitrogen, Camarillo, CA, USA) and transfected to SH-SY5Y cells by the calcium phosphate method or lipofection [29,30]. The transfected cells were maintained in DMEM containing 10% fetal bovine serum, and stably transfected cells selected by hygromycin B-containing medium. AβPP and PS1-double transfected cells were described in our previous report [31]. For treatment with the apoptosis-inducing agents to induce apoptosis, cultured cells at >70% confluency were treated with hydrogen peroxide (H_2O_2) at 0, 0.1, 0.3 and 0.5 μM , MG132 (Biomol, Plymouth Meeting, PA, USA), a proteasome inhibitor, at 0, 0.1, 0.3 and 0.5 nM, or etoposide (ETP; Sigma), a topoisomerase II inhibitor, at 0, 10, 50 and 100 nM for 24 h (H_2O_2 or MG132) or 48 h (ETP). To inhibit Aβ generation, cells were treated with a β-site AβPP-cleaving enzyme (BACE) inhibitor (β-secretase inhibitor III; Calbiochem, San Diego, CA, USA) and γ-secretase inhibitor (γ-secretase inhibitor X; Calbiochem, San Diego, CA, USA) for 24 h at concentrations of 0, 1 and 5 μM for BACE [32] and 0, 0.5 and 1 μM for γ-secretase [33].

Reverse Transcriptase-Polymerase Chain Reaction (RT-PCR)

Cells were lysed and total RNA was prepared using RNeasy columns (Qiagen, Hilden, Germany). For quantitative RT-PCR assays, 1 μg of total RNA was applied to cDNA synthesis using a First-strand Synthesis Kit (Roche, Basel, Switzerland), and one-twentieth of the resulting cDNA product was amplified by PCR (Perkin Elmer, Waltham, MA, USA). The primers for PCR were: human p53: forward, 5'-CGC ACA GAG GAA GAG AAT CTCC-3' and reverse, 5'-CTG GGC ATC CTT GAG TTC CAA GGC-3'; human β-actin: forward, 5'-TGG GCA TGG AGT CCT GTG GCAT-3' and reverse, 5'-CCG GAC TCG TCA TAC TCC TGC TTG-3'. Initially, the cDNAs were denaturated at 94 °C for 1 min, followed by annealing at 53 °C (p53) or 60 °C (β-actin) for 1 min and extension at 72 °C for 1 min. The amplified products were electrophoresed in a 2.5% agarose gel, followed by densitometric analysis using the NIH Image 1.62b7 software, and were corrected by β-actin signal intensities.

Western blotting of PS1, p53 and β-actin

Cells were lysed in 2% sodium dodesylsulfate (SDS), and the resulting protein concentrations were measured using a BCA Protein Assay Reagent Kit (Pierce, Rockford, IL, USA). The total protein concentrations were adjusted, and 20 μg of protein from each sample was resolved in loading buffer (100 μM Tris-HCl pH6.8, 12% 2-mercaptoethanol, 20% glycerol, 4% SDS, 0.01% Bromophenol Blue), electrophoresed in an SDS-15% polyacrylamide gel and electro-transferred onto a PVDF membrane (Millipore, Bedford, MA, USA). The membrane was blocked with 5% skim milk in TBST (25 μM Tris-HCl pH7.6, 150 μM NaCl, 0.1% Tween-20) for 1 h and then incubated with anti-p53 polyclonal (1:500 dilution; FL393; Santa Cruz, CA, USA), anti-PS1 N-terminal polyclonal (1:5,000 dilution; H-70; Santa Cruz, CA, USA) or anti-β-actin monoclonal (1:1,000 dilution; Sigma) primary antibodies

in TBST for 2 h at room temperature. After washing in TBST, the membrane was incubated with the appropriate horseradish peroxidase-conjugated secondary antibody (1:1,000 dilution; Vector Lab, Burlingame, CA, USA) in TBST for 1 h, and antigen-antibody complexes were detected using an ECL Western Blotting Detection Reagent System (Amersham Bioscience, Piscataway, NJ, USA). The relative amounts of p53 protein were measured by densitometric analysis using the NIH Image 1.62b7 software, and were corrected by β-actin signal intensities.

Western blotting of intracellular and extracellular Aβ

Intracellular Aβ was detected by western blot using a procedure similar to our previous report [31]. Cells were homogenized in TBS (25 μM Tris-HCl pH7.6, 150 μM NaCl) containing protease inhibitors. Postnuclear supernatant fractions were collected by centrifugation at 600 g for 15 min at 4°C. Each sample containing 400 μg of protein was further centrifuged at 100,000 g for 1 h. The pellets were solubilized in 70% formic acid and incubated at 4°C overnight, followed by drying in a centrifugal concentrator. Pellets were washed with chloroform/methanol [2:1 (v/v)] and dried again. Samples were solubilized in sample buffer (10% glycerol, 8% SDS, 0.1 M Tris-HCl pH 6.8, 4% 2-mercaptoethanol, 0.01% Bromophenol Blue) containing 8 M urea and subjected to Tris-Tricine SDS-polyacrylamide gel electrophoresis. Proteins were transferred onto a PVDF membrane (Millipore, Bedford, MA, USA). The membrane was incubated in 2.5% glutaraldehyde for 30 min at room temperature and washed with PBS containing 50 μM monoethanolamine for 5 min, followed by boiling in PBS. This procedure enhanced Aβ immunoreactivity dramatically. The membrane was incubated with anti-Aβ1-16 antibody, 6E10 (1:1,000 dilution; Biocompare, South San Francisco, CA, USA), in TBST at 4°C overnight, followed by incubation with anti-rabbit secondary antibody (1:5,000 dilution; Vector Lab, Burlingame, CA, USA) in TBST for 1 h at room temperature. Specific 4-kD bands were detected using a highly sensitive detection kit, the SuperSignal West Dura Extended Duration Substrate (Pierce, Rockford, IL, USA). Extracellular Aβ in the medium was collected by immunoprecipitation and detected by western blotting using a method according to a previous report [34]. Briefly, 25 μl of Dynabeads Protein G (Invitrogen, Camarillo, CA, USA) and 5 μg of an anti-Aβ antibody (4G8, Biocompare, South San Francisco, CA, USA) were added into 1 μl of 24-h conditioned medium and 250 μl of 5X RIPA buffer (2.5% Nonidet P-40, 1.25% sodium deoxycholate, 0.25% SDS, 750 μM NaCl, 250 μM HEPES, pH 7.4) containing protease inhibitor mixture Complete^{TM} Mini (Roche Applied Science Japan, Tokyo, Japan), and were incubated under rotation for 1 h at 4°C. Collected Aβ was eluted by 20 μl of loading buffer with boiling, followed by western blotting with an anti-Aβ antibody (6E10) using an ECL Western Blotting Detection Reagent System (Amersham Bioscience, Piscataway, NJ, USA).

Proteasome activity assay

Proteasome activity was measured according to a previous report [35] with a minor modification. Briefly, cells were lysed in water with sonication, and the total protein concentration in the supernatant was measured using a BCA Protein Assay Reagent Kit (Pierce, Rockford, IL, USA). The proteasome activity in 10 μg of protein in each sample was measured using a 20S Proteasome Assay Kit (SDS-activation format; Boston Biochem, Cambridge, MA, USA). Briefly, 0.03% SDS was used to activate the proteasome in soluble fraction, and the activated proteasome cleaved Suc-Leu-Leu-Val-Tyr-AMC to generate a fluorescent product (AMC). The fluorescence was measured every 10 min for 2 h at 37°C using an MTP-800AFC multi-microplate reader (Corona Electric Japan, Tokyo, Japan) with wavelengths of 380 nm (excitation) and 460 nm (emission).

Statistical analysis

All data obtained from at least three independent experiments were expressed as the mean ± SD. Differences between two groups were statistically analyzed by an unpaired two-tailed Student's t-test. For multiple comparisons, two-factor ANOVA followed by Bonferroni post hoc analysis was used. Values of $p < 0.05$ were considered to indicate statistical significance.

RESULTS

Appropriate cycles of amplification for RT-PCR assay

First, we checked PS1 expression in the PS1-transfected cells by western blot. As shown in Fig. 1, approximately 50-kD full-length PS1 was detected in wild-type, I143T-mutant and G384A-mutant PS1-

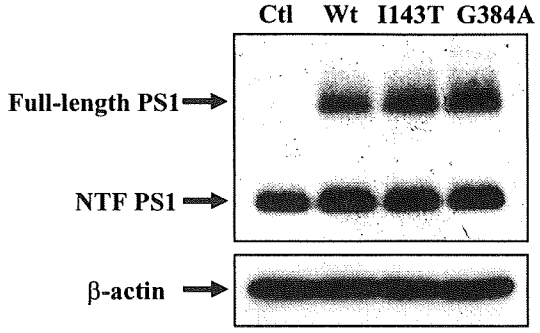

Fig. 1. Western blot analysis of PS1 and β-actin. Full-length PS1 bands were detected in wild-type (Wt), I143T-mutant and G384A-mutant PS1-transfected cells but not in control (Ctl) cells, which were transfected with vector only. Also, N-terminal fragment (NTF) of PS1 were increased in Wt, I143T-mutant and G384A-mutant PS1-transfected cells but not in control cells.

transfected cells but not in control cells transfected with vector only. Also, approximately 30-kD N-terminal fragment of PS1 was increased in the PS1-transfected cells, which was the same as described in a previous report [30]. Thus, exogenous PS1 proteins were expressed at similar levels in those cells. Next, we determined the linear-increase phases of the PCR cycle numbers for p53 and β-actin. Each PCR amplification was stopped at 17, 20, 23, 25, 27, 30 and 33 cycles. Cycles from 23 to 27 for p53 cDNA (Fig. 2A) and cycles from 20 to 27 for β-actin cDNA (Fig. 2B) were found to be the linear-increase phases, and cycles over 30 reached a plateau phase. Thus, we selected the 25-cycle point for our semi-quantitative RT-PCR studies.

Baseline levels of p53 protein, but not mRNA, are increased by PS1 mutants

We examined the baseline levels of p53 mRNA and protein using RT-PCR and western blotting, respectively. Although the p53 mRNA levels were not elevated in mutant PS1-transfected cells compared to wild-type PS1-transfected cells (Fig. 3A), the p53 protein levels were significantly increased in mutant PS1-transfected cells (Fig. 3B). The p53 protein level was elevated more significantly in G384A-mutant PS1-transfected cells ($\sim$200%, $p < 0.01$) than in I143T-mutant PS1-transfected cells ($\sim$150%, $p < 0.05$).

Increasing levels of p53 protein are enhanced by PS1 mutants when treated with three apoptosis-inducing agents

We studied the effects of the PS1 mutants on p53 expression during the process of apoptosis. In our other report [28], we demonstrated that decreases in cell viability were enhanced in mutant PS1-transfected cells after treatment with 0.5 nM MG132 (24 h), 100 nM ETP (48 h) or 0.7 μM H_2O_2 (6 h). We here examined the changes in the p53 mRNA and protein levels after treatments with these three agents at similar concentrations for 24 h (MG132 or H_2O_2) or 48 h (ETP). After treatment with 0.5 nM MG132, the p53 mRNA levels were decreased in G384A-mutant PS1-transfected cells compared to wild-type PS1-transfected cells, but the differences did not reach statistical significance (Fig. 4A). In contrast, increases in the p53 protein level were significantly enhanced in mutant PS1-transfected cells (Fig. 4B). After treatment with 100 nM ETP, there was a tendency toward unchanged or slightly increased p53 mRNA expression levels in mutant PS1-transfected cells (Fig. 5A), while increases in the p53 protein level were significantly enhanced in mutant PS1-transfected cells (Fig. 5B). Similar alterations in the p53 mRNA and protein levels were observed after treatment with H_2O_2 (Fig. 6). Thus, enhancement of increases in the p53 protein but not mRNA levels may be a common effect of these PS1 mutants after treatment with apoptosis-inducing agents. Alteration patterns were basically the same in control and wild-type PS1-transfected cells (Fig. 6), which indicates that p53 mRNA expression would be slightly enhanced in mutant PS1-transfected cells.

Increases in the p53 protein levels by PS1 mutants are counteracted by BACE and γ-secretase inhibitors

To check the possibility that Aβ overproduction is involved in aberrancy of the p53 protein expression, we treated the cells with a BACE inhibitor and γ-secretase inhibitor. First, we checked alteration of intracellular Aβ and p53 protein levels when treated with H_2O_2, and evaluated effects of these inhibitors on intracellular and extracellular Aβ levels. We used AβPP and PS1-double transfected cells [31], since intracellular Aβ was detectable only in AβPP-transfected cells. After treatment with H_2O_2, intracellular Aβ, most of which may be Aβ_{42} [11], was slightly increased, and p53 protein was increased correlatively (Fig. 7A). Treatment with the BACE inhibitior or γ-secretase inhibitor lowered the intracellular Aβ levels apparently in these cells (Fig. 7B). Similar effects of secretase inhibitors on extracellular Aβ levels were observed (Fig. 7C). Next, treatment with both secretase inhibitors significantly lowered the baseline p53 protein levels in mutant PS1-transfected cells to similar levels to those in

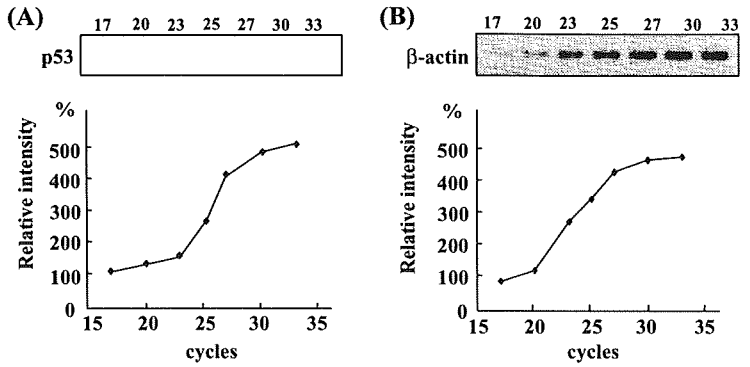

Fig. 2. RT-PCR analysis of p53 and β-actin cDNA amplification. (A) Amplification of p53 cDNA at 17, 20, 23, 25, 27, 30 and 33 PCR cycles (upper) and relative densities of the PCR products at each cycle (lower). (B) Amplification of β-actin cDNA at 17, 20, 23, 25, 27, 30 and 33 PCR cycles (upper) and relative densities of the PCR products at each cycle (lower).

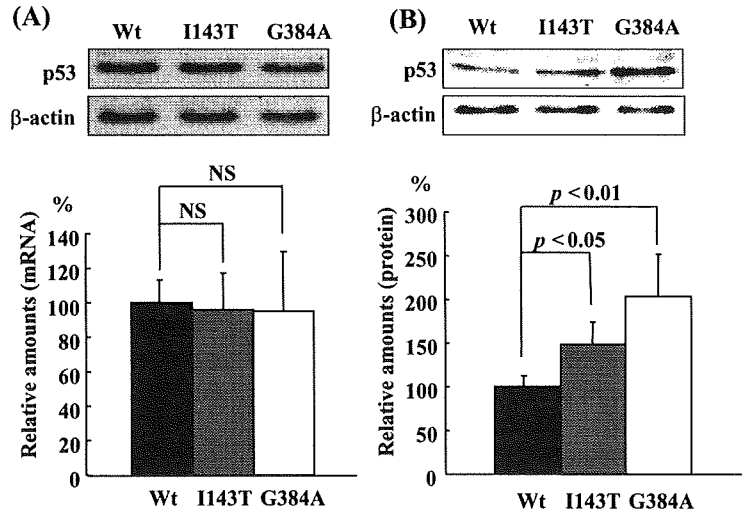

Fig. 3. RT-PCR and western blot analysis of baseline p53 mRNA and protein levels in wild-type (Wt) and I143T- or G384A-mutant PS1-transfected cells. (A) RT-PCR analysis of p53 and β-actin (upper) and relative amounts of the PCR products amplified from p53 mRNA (lower). Values are expressed as relative levels compared to wild-type PS1-transfected cells ($n = 5$). (B) Western blotting analysis of p53 and β-actin (upper) and relative amounts of p53 protein (lower). Values are expressed as relative levels compared to Wt PS1-transfected cells ($n = 5$). NS: not significant.

wild-type PS1-transfected cells ($p < 0.05$) (Fig. 8). Moreover, increases in the p53 protein levels after treatment with H_2O_2 were significantly attenuated by treatment with the BACE or γ-secretase inhibitors (Fig. 9). These results were in good agreement with our other observation that these secretase inhibitors suppressed caspase-3/7 activation by H_2O_2 treatment in mutant PS1-transfected cells [28].

Decreases in proteasome activity by PS1 mutants

Since the UPS is the major compartment that regulates p53 degradation and may be affected by intracellular Aβ [35], we assessed the intracellular proteasome activity in these transfected cells. As shown in Fig. 10A, fluorescence of the substrate (AMC) was gradually produced by proteasomal cleavage, and the rate of increase in fluorescence was lower in mutant PS1-transfected cells. The increasing slope of the curve, which represented the relative proteasomal activity, was calculated by the linear regression analysis. The relative proteasome activity, ΔAFC, was significantly decreased in mutants PS1-transfected cells compared to wild-type PS1-transfected cells ($p < 0.05$, Fig. 10B). In addition, the relative proteasome activity was significantly decreased in AβPP and G384A-

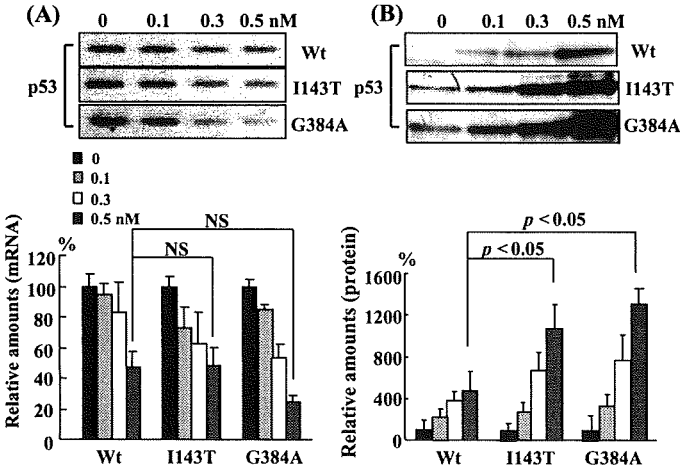

Fig. 4. RT-PCR and western blot analysis of p53 mRNA and protein levels in wild-type (Wt) and I143T- or G384A-mutant PS1-transfected cells after treatment with MG132 for 24 h. (A) RT-PCR analysis of p53 (upper) and relative amounts of the PCR products amplified from p53 mRNA (lower). Values are expressed as relative levels compared to wild-type PS1-transfected cells ($n = 3$). (B) Western blotting analysis of p53 (upper) and relative amounts of p53 protein (lower). Values are expressed as relative levels compared to untreated cells in each group ($n = 3$). NS: not significant.

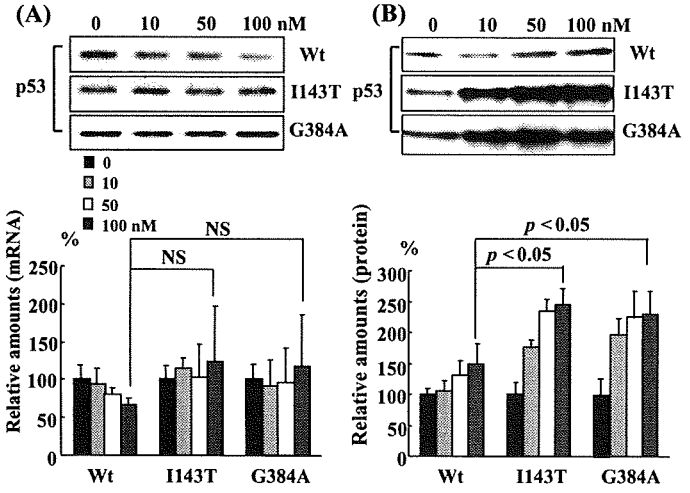

Fig. 5. RT-PCR and western blot analysis of p53 mRNA and protein in wild-type (Wt) and I143T- or G384A-mutant PS1-transfected cells after treatment with ETP for 48 h. (A) RT-PCR analysis of p53 (upper) and relative amounts of the PCR products amplified from p53 mRNA (lower). Values are expressed as relative levels compared to wild-type PS1-transfected cells ($n = 3$). (B) Western blotting analysis of p53 (upper) and relative amounts of p53 protein (lower). Values are expressed as relative levels compared to untreated cells in each group ($n = 3$). NS: not significant.

mutant PS1-double transfected cells compared to cells transfected with G384A-mutant PS1 only ($p < 0.05$, Fig. 10B).

DISCUSSION

PS1 and PS2 have been reported to regulate neuronal survival and death, and their gene mutations are involved in the pathogenesis of AD due to aberrations in the cleavage of many transmembrane proteins, including AβPP, calcium homeostasis in ER, and β-catenin turnover [19,36]. In this report, we demonstrated that p53 expression was enhanced in mutant PS1-transfected cells at baseline as well as when treated with apoptosis-inducing agents. These data are consistent with some former reports that have demonstrated involvement of *PS1/2* gene mutations in p53 mRNA ex-

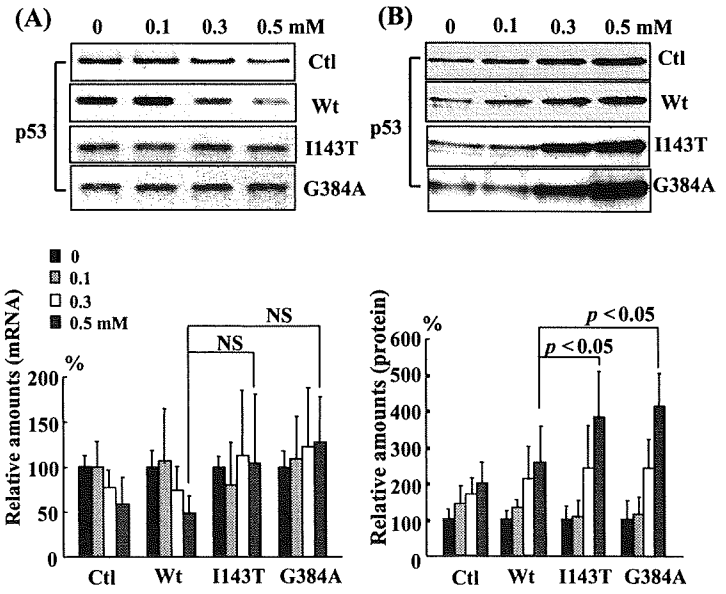

Fig. 6. RT-PCR and western blot analysis of p53 mRNA and protein in control (Ctl), wild-type PS1-transfected (Wt), I143T-mutant PS1-transfected and G384A-mutant PS1-transfected cells after treatment with H_2O_2 for 24 h. (A) RT-PCR analysis of p53 (upper) and relative amounts of the PCR products amplified from p53 mRNA (lower). Values are expressed as relative levels compared to WT-PS1 cells ($n = 3$). (B) Western blotting analysis of p53 (upper) and relative amounts of p53 protein (lower). Values are expressed as relative levels compared to untreated cells in each group ($n = 3$). NS: not significant.

pression [22,24,37]. However, our present data suggest an alternative mechanism by which I143T- and G384A-mutant PS1 increase p53 protein levels. We reported that intracellular Aβ was increased by treatment with H_2O_2 or ETP in cultured neurons [11]. Intracellular Aβ has recently been reported to induce various pathological effects [38], and impairment of proteasome activity may be one of the pathogenesis [35]. In fact, we found that AβPP and G384A-mutant PS1-double transfection attenuated proteasome activity more remarkably than G384A-mutant PS1 transfection only, which indicates that Aβ overproduction may affect proteasome activity. Also, we observed attenuation of proteasome activity by treatment with H_2O_2, which may support this concept (data not shown). Although we reported that p53 mRNA expression was increased in the L286V-mutant PS1-transgenic mice [22], only a small increase of p53 mRNA expression in mutant PS1-transfected cells was found when treated with ETP or H_2O_2. Such different effects among PS1 mutants may be due to variation of intracellular Aβ accumulation sites, or due to different effects on cleavage of AB-DIP that regulates translocation of Aβ to nucleus [23].

P53 is involved in both intrinsic and extrinsic apoptosis pathways, i.e., the mitochondrial and Fas-mediated pathways [25]. In addition, p53 has been reported to contribute to apoptosis caused by ER stress [39]. In the view of activation of initiator caspases, we demonstrated that ER stress, Fas receptor-mediated extrinsic pathway, and a mitochondrial pathway may be all involved in the enhancement of apoptosis in these mutant PS1-transfected cells [28]. Therefore, fundamental elevation of p53 protein levels may accelerate multiple apoptosis pathways in mutant PS1-transfected cells. Although BACE and γ-secretase inhibitors counteracted p53 protein upregulation in the present study and attenuated caspase-3/7 activity in our other study [28], the concentration of γ-secretase inhibitor required to attenuate caspase-3/7 activity (5 μM) was higher than the concentration required to attenuate p53 expression (1 μM). In addition, attenuation of p53 protein increase by γ-secretase inhibitor seemed more completely than by BACE-inhibitor when treated with H_2O_2 (Fig. 9). Thus, aberrant γ-secretase activity may be multi-pathogenic, contributing to Aβ-related/-unrelated p53 upregulation and even p53-unrelated apoptosis signaling pathways.

Although p53 is widely known to induce cell cycle arrest, aberrant shift to mitotic stage of the neurons in AD is suggested. Recently, a combination of mitotic changes (hit 1) and oxidative stress (hit 2) are suggested to be early events in the pathogenesis of AD, which is called "the two-hit hypothesis" [40]. When oxidative stress (hit 2) promotes intracellular Aβ_{42}-related p53

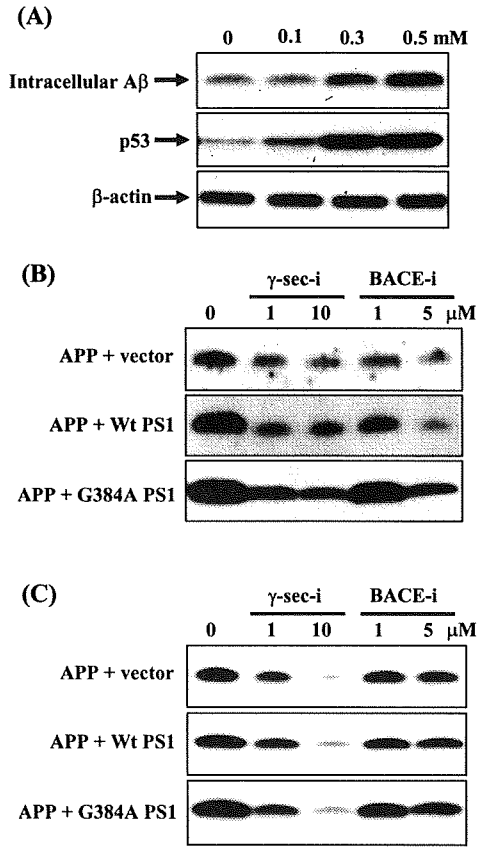

Fig. 7. Western blot analysis of intracellular Aβ, p53 and β-actin in AβPP+G384A-mutant PS1-double transfected cells after treatment with H_2O_2 for 24 h (A). Western blot analysis of intracellular Aβ (B) and extracellular Ab (C) in cultures of AβPP and PS1-double transfected cells after treatments with inhibitors of γ-secretase or BACE for 24 h. BACE-i: BACE inhibitor; γ-sec-i: γ-secretase inhibitor.

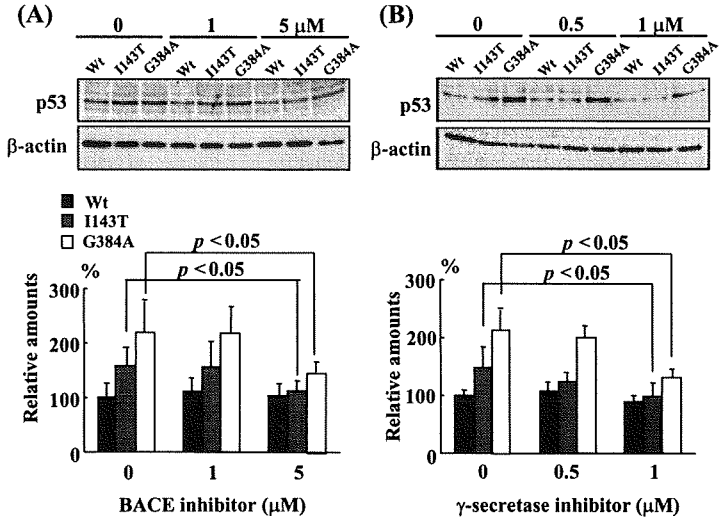

Fig. 8. Western blot analysis of baseline p53 protein levels in wild-type (Wt) and I143T- or G384A-mutant PS1-transfected cells after treatment with inhibitors of BACE (A) or γ-secretase (B) for 24 h. Western blotting analysis of p53 and β-actin (upper) and relative amounts of p53 protein (lower). Values are expressed as relative levels compared to untreated Wt PS1-transfected cells ($n = 3$).

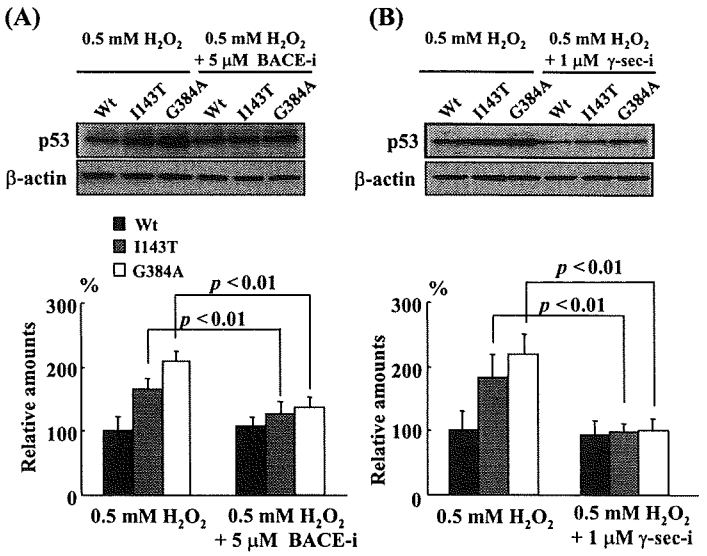

Fig. 9. Western blot analysis of p53 protein levels in wild-type (Wt) and I143T- or G384A-mutant PS1-transfected cells after treatment with H_2O_2 and inhibitors of BACE (A) or γ-secretase (B) for 24 h. Western blotting analysis of p53 and β-actin (upper) and relative amounts of p53 protein (lower). Values are expressed as relative levels compared to Wt PS1-transfected cells ($n = 3$). BACE-i: BACE inhibitor; γ-sec-i: γ-secretase inhibitor.

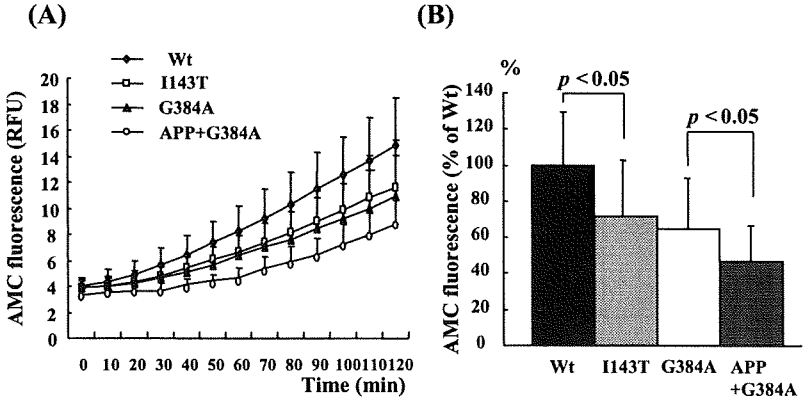

Fig. 10. Proteasome activities in wild-type (Wt), I143T-mutant and G384A-mutant PS1-transfected cells and AβPP+G384A-mutant PS1-double transfected cells. (A) Time-course measurements of AMC fluorescence generated by proteasomal degradation of a specific substrate ($n = 11$). Proteasome activities are expressed as relative fluorescence units (RFU) /μg protein /min. (B) Relative rates of increase in the AMC fluorescence represent the relative proteasome activity ($n = 11$).

upregulation, conflict of acceleration (hit 1) and braking (hit 2) of cell cycle may result in apoptosis of numerous neurons. Subsequently, neuronal apoptosis may release aggregated Aβ into extracellular space [41], leading to further extracellular Aβ toxicity.

Recently, Billings and colleagues [42] have demonstrated that disappearance of intraneuronal $A\beta_{42}$ improved memory dysfunction in 3XTg, a PS1-related FAD mouse model. More recently, transgenic mice with five FAD mutations (5XTg) have been found to show intraneuronal $A\beta_{42}$ accumulation starting at 1.5 months of age, prior to plaque formation [10]. In addition, the aberrant frameshift protein UBB^{+1}, which inhibits the UPS, was reported to accumulate in the pathologic hallmarks of AD [43], whether in sporadic AD brains [44] or in FAD brains including those with I143T and G384A *PS1* gene mutations [45]. Thus, if the UPS is impaired by UBB^{+1} in AD, proteasome activity may be further inhibited by $A\beta_{42}$ overproduction and may accelerate p53 accumulation in FAD patients with I143T and G384A *PS1* gene mutations. Although many other mutations in the *PS1* and *PS2* genes remain